Available online at www.sciencedirect.com

ScienceDirect

Procedia CIRP 81 (2019) 1376–1381

www.elsevier.com/locate/procedia

52nd CIRP Conference on Manufacturing Systems

Effect of Extrusion Temperature on Printable Threshold Overhang in Additive Manufacturing

Jingchao Jiang, Xun Xu*, Jonathan Stringer

Department of Mechanical Engineering, University of Auckland, Auckland, 1142, New Zealand

* Corresponding author. *E-mail address:* xun.xu@auckland.ac.nz

Abstract

Despite of additive manufacturing technologies being rapidly developed with wide applications in the fields of aerospace, engineering, medical application and marine, support structures are still unavoidable for many printed products with overhangs, resulting in extended build time and expensive post-processing, material waste, and sometimes failure to fabricate the part of the required quality. The threshold overhang angle that can be self-supported is generally set at 45° for FDM printers. However, different process parameters such as extrusion temperature and print speed can also have a great impact on printable threshold overhang angle (PTOA). In this paper, the influence of extrusion temperature on PTOA is studied theoretically and experimentally for the achievement of the lowest possible PTOA. First, theoretical analysis of overhang with regard to extrusion temperature is carried out. Then experiments of overhangs with 20°, 30°, 40° and 50° in extrusion temperatures of 175 °C, 190 °C, 205 °C and 220 °C are conducted on an FDM printer. According to the results, PTOA can be quite different under various extrusion temperatures and the theoretical analysis can be used for predicting the lowest PTOA. The findings can also provide some references for future research in high-precision printing by adjusting relevant print parameters.

Peer-review under responsibility of the scientific committee of the 52nd CIRP Conference on Manufacturing Systems.

Keywords: additive manufacturing; support structure; printable threshold overhang angle; surface quality

1. Introduction

Additive manufacturing (AM) technology, also known as 3D printing, rapid prototyping or direct digital manufacturing, was first developed in 1987 by 3D Systems [1]. It has been rapidly developed with wide applications in the fields of aerospace, engineering, medical application and marine. Though AM has been reckoned as a sustainable and environmental-friendly technology due to its layer-by-layer nature and consequent lack of material wastage, attentions are still being paid to further reduce the energy consumption and impact on environment in AM processes [2,3]. The manufacturing process starts from the bottom of a part and continues successively layer by layer to the top, resulting in problems for overhangs that cannot be printed as there is no supporting layer beneath them [4]. Support structures have to be manually discarded after printing, thus wasting the material used for support and increasing the cost of post-processing; it is, however, inevitable that support structures have to be printed for extrusion-based processes where extreme overhangs exist.

A lot of research has been carried out to reduce the use of support materials for saving cost and time needed for printing or post-processing [5–9]. Altering the print orientation of parts for reducing the support volume has been investigated by many researchers [10–12]. Another strategy to save cost and improve finished surface quality is to build supports with different materials which are soluble or sacrificial. This means using the part material to build the final object while using another sacrificial material (either cheaper than the part

Peer-review under responsibility of the scientific committee of the 52nd CIRP Conference on Manufacturing Systems.
10.1016/j.procir.2019.04.047

material or easier to remove) to print the support when manufacturing a part. In AM processes, the most widely used soluble support materials are polymer feedstocks which are soluble in relatively benign solvents such as water (poly(vinyl alcohol)) and limonene (high impact poly(styrene)). Another common combination is a part printed with acrylonitrile butadiene styrene (ABS) while a sacrificial support structure printed with polylactic acid (PLA) [13]. Hopkins et al. [14] developed a support material containing acrylic copolymers with a polymeric impact modifier. The new support material can effectively resist breaking or cracking, and can be removed easily and quickly. In an alkaline aqueous solution, the material can be dissolved rapidly. Ni, Wang and Zhao [15] also carried out some research on Poly(vinyl alcohol) (PVA) which can act as water-soluble supports in AM processes.

Adopting cellular/lattice or other better structures as support is another method for further reducing the support consumption. As the advantage of their low volume fraction, cellular structures provide opportunities to reduce the volume of support materials and allow for easy removal of support structure as well as manufacturing time. Vaidya and Anand [16] employed Dijkstra's shortest path algorithm [17] to generate cellular support structures. Strano et al. [18] proposed a new approach which applies a new optimisation algorithm to use pure mathematical 3D implicit functions for the design and generation of the cellular support structures including graded supports. Lu et al. [19] applied the Voronoi diagram to compute irregular honeycomb-like volume tessellations which define the inner structure. They took honeycomb-cell structure as inner support structures based on a hollowing optimization algorithm. Tree-like support structure methods were researched by two publications [20,21].

Apart from all the methods proposed above, another potential way to reduce the support consumption and cost is by setting the printable threshold overhang angle (PTOA) as small as possible to reduce the support area. PTOA means an overhang with a lowest angle that can be fabricated without adding support during the deposition process. In this paper, the overhang angle (β) is defined as the angle between the x-y plane (i.e. the build platform) and the overhang surface tangent in the x-z (or y-z) plane (Fig.1). The lower the PTOA, the less the support area. Generally, PTOA is set at 45° in most printers [22]. Some also take a test first to determine the angle size as it may be different according to printers and materials [23]. However, little attention has been paid to seek the lowest PTOA by adjusting relevant parameters. Mertens et al. [24] may be the first who carried out some research in this aspect. They optimized the degree of overhang angle under different parameters in Selective Laser Melting by testing 60°, 45° and 30° under various laser power. Wang, et al. [25] investigated the surface quality of the curved overhanging structure manufactured from 316-L stainless steel by SLM under different laser scanning energy input. However, both of these two studies did not focus on extrusion-based AM techniques.

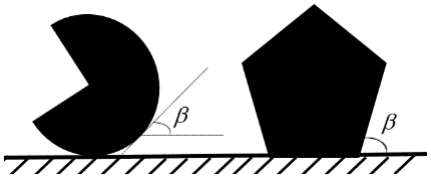

Fig. 1. Definition of overhang angle (β) in this paper.

In this paper, theoretical analysis and experimental study are carried out to study extrusion temperature's effect on PTOA in extrusion-based 3D printing processes. This is a potential way to lower PTOA as much as possible by improving print settings, thus achieving time- and cost-savings.

2. Theoretical analysis

In an extrusion-based 3D printing process, the phase of thermoplastic material is in 'liquid' when in or just extruded from the nozzle. The final shape of this 'liquid' filament will be influenced by viscosity and elastic stresses, surface tension and inertia before solidification [26,27]. It is hypothesized that the surface roughness in different overhang angle sizes are seen as a reflection of such free-surface flows. The printed fluid material has the phenomenon of "self-thinning", in which no external driving force is imposed (or in which the internal dynamics that develop spontaneously in the fluid are much faster than any external forcing). In such flows the fluid jet, thread, film or sheet thins down and breaks up naturally under the action of capillary forces [28]. In an extrusion-based 3D printing process, the melted material is similar to the above situation. Therefore, the viscous time scale (t_v) of a printed material and the solidification timescale (t_s) will influence the self-thinning and break-up phenomenon of the printed 'liquid' material, which is seen as the main reason of collapsed/deformed/distorted surface of overhang in different angle sizes. The equation of a viscous time scale is as follows [28],

$$t_v \approx \frac{\eta l}{\delta} \tag{1}$$

where t_v is viscous time scale, η is viscosity, l is length scale of the flow and $\delta$is surface tension of a fluid. At the same time, the solidification timescale $t_s$can be estimated as:

$$t_s = \frac{D^2}{\alpha \tan^2 \beta}\left(\frac{T_i - T_S}{T_S - T_b}\right) \tag{2}$$

$$\alpha = \frac{k}{\rho C} \tag{3}$$

where k is thermal conductivity, ρ is density of material, C is heat capacity of material, D is nozzle diameter, α is thermal diffusivity, β is overhang angle size, $T_i$is print temperature, T_S is the solidification temperature and T_b is bed temperature.

3. Experimental study

3.1. Equipment

A Kossel Delta 3D printer was used in this study from Shenzhen Anycubic technology co., LTD. The build area

shape is circular with diameter of 180 mm and maximum height of 300mm. The nozzle diameter used was 0.4 mm. PHYSICA UDS 200 and DSC Q1000 were used for measuring material properties (solidification temperature, thermal conductivity and heat capacity).

3.2. Material

The material used for printing in this study is PLA. PLA is considered as the most common biopolymer among 3D printing materials known due to its mechanical properties such as good stiffness and strength, its low toxicity, recyclability, compostable with the environment and the fact that CO_2 emissions can be significantly reduced when it is produced from renewable resources. The diameter of this filament is 1.75 mm, with extrusion temperature between 175-220 °C.

3.3. Experimental settings

Before printing, the 3D part needs created and sliced into layers in G-code format. Slicer software Cura 15.04 was used for slicing digital models in this study. The settings of this printer are shown in Table 1. The original models are designed by Solidworks and displayed in Fig.2 with angle sizes of 20°, 30°, 40°, 50° and the same height of 35 mm. The diameter of the pillars is 10mm. Based on these settings, the following 4 groups of experiments (Table 2) were set and carried out accordingly with a sample size of 5.

Table 1. Print parameter settings.

Layer height (mm)	0.2
Shell thickness (mm)	0.8
Bottom/top thickness (mm)	1
Fill density (%)	0
Support type	No support

Table 2. Experimental settings of each group.

	Overhang angle size (°)	Extrusion temperature (°C)	Cooling fan speed (RPM)	Print speed (mm/s)
Group 1	20	175, 190, 205, 220	250	30
Group 2	30			
Group 3	40			
Group 4	50			

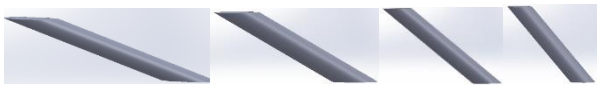

Fig. 2. Original models with angle sizes of 20°, 30°, 40° and 50° (left to right, respectively).

4. Results and analysis

In order to better compare these results, image-based analysis was carried out as the program of Fig. 3 shows. Specifically, each photo of the printed overhang was analysed by NI vision assistant and Engauge Digitizer 4.1, respectively. After obtaining the downfacing surface contour of each printed overhang, surface roughness value was calculated by MATLAB for comparing the surface quality of overhangs printed in different parameters. The surface roughness value applied in this paper is the surface roughness average (Ra). The value is defined as the arithmetic average deviation from the measurement centreline to the surface profile [29]. The rule of determining the centreline is that the total area between the centreline and above contour is the same as the total area between the centreline and below contour. All surface roughness of the printed 80 parts are calculated and the mean values of Ra in every condition are displayed in Table 3. The standard deviations among five Ra values in each condition are shown in the brackets next to the mean Ra. As can be seen, the standard deviations are very small, which means the experiments are reliable and repeatable.

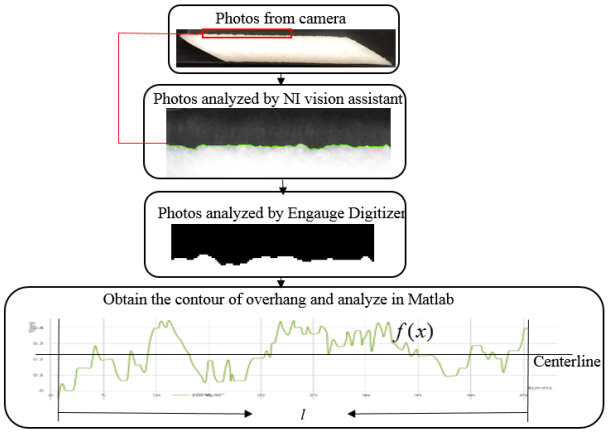

Fig. 3. Analysis program of overhangs.

Table 3. Mean Ra (Unit: mm) of overhangs in different conditions.

Angle size \ Extrusion temperature	220°C	205°C	190°C	175°C
50°	0.307	0.163	0.125	0.057
	(0.020)	(0.018)	(0.015)	(0.012)
40°	0.362	0.269	0.149	0.109
	(0.021)	(0.017)	(0.014)	(0.010)
30°	0.475	0.406	0.331	0.152
	(0.025)	(0.023)	(0.019)	(0.012)
20°	1.220	0.933	0.673	0.510
	(0.045)	(0.039)	(0.031)	(0.029)

However, the nature of 3D printing process will induce stair-step effect which is also a reason of resulting in surface roughness as shown in Fig. 4(a). The surface roughness of the theoretical overhang models in different angle sizes are calculated as shown in Fig. 4(b). The theoretical minimum surface roughness can be calculated as follows,

$$Ra = \frac{\frac{1}{4}w_i h_i}{\frac{w_i}{\cos\beta}} = \frac{1}{4}h_i \cos\beta \quad (4)$$

The results of theoretical Ra in different overhang angle sizes are listed in Table 4. As can be seen from this table, all

theoretical surface roughnesses are lower than the measured ones of Table 3, with minor changes within different angle sizes.

Table 4. Theoretical Ra of overhangs in different angle sizes based on 3D models.

Overhang angle size	20°	30°	40°	50°
Theoretical Ra (mm)	0.047	0.043	0.038	0.032

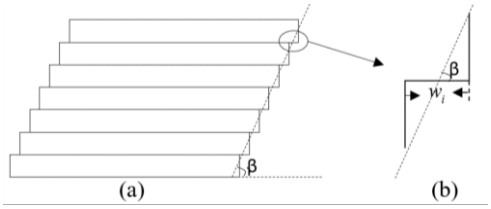

Fig. 4. (a) stair-step effect in 3D printing; (b) Simplified model for calculating theoretical surface roughness.

As can be seen from Table 3 and Fig. 5, overhangs with larger angle size get better surface quality (less surface roughness). The surface roughness of 220 °C, 20° overhang arrives at 1.220 mm while it is only 0.307 mm for 220 °C, 50° overhang. The larger the overhang angle size is, the less the surface roughness could be. When the surface roughness is acceptable (depending on the requirement of the product) in some angle size, higher overhang angle sizes will not need support while lower sizes will have to use support for getting satisfactory surface quality. This is also the reason why a slicing software needs to have a threshold overhang angle for generating support area.

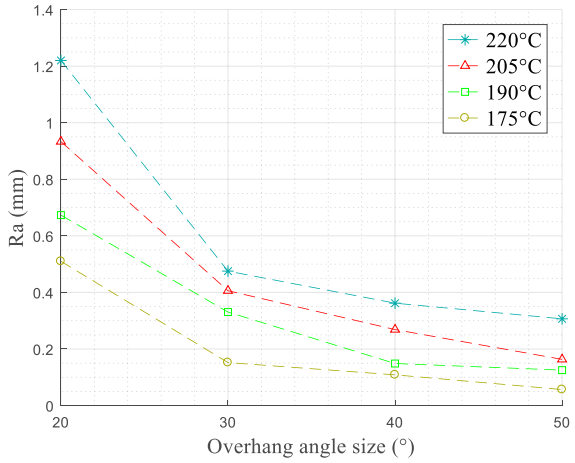

Fig. 5. Mean Ra for different overhang angle sizes at different extrusion temperatures.

According to the experiment results, extrusion temperature is an important factor of surface quality of a printed overhang, thus influencing PTOA. Taking angle 30° under 175 °C and 220 °C as an example in Fig. 6, the finished part of 175 °C is better than that of 220 °C in terms of the surface resolution. As can be seen from Fig. 5, overhang with higher extrusion temperature has worse surface quality (higher surface roughness). This means PTOA can be changed by altering extrusion temperature when other conditions are the same and the same surface quality can be achieved. According to the experiment results, the lower temperature would be better for achieving lower PTOA. However, the allowed lowest extrusion temperature should be determined first as clogging or difficulty of extruding the filament may occur if extrusion temperature is too low, as well as slipping between the filament and pinch rollers. In addition, as shown in the literature [30], the printed strength/solidity/quality will be influenced by print parameters, including extrusion temperature. There should be a trade-off between surface quality and strength, etc. in the future. However, in this paper, only surface roughness is considered for achieving the lowest PTOA.

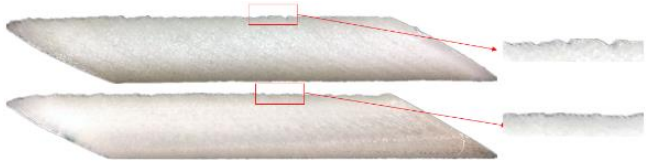

Fig. 6. Printed parts with 175 °C, 30° (bottom) and 220 °C, 30° (top).

5. Discussion

As stated in the theoretical section, t_s/t_v is used as a reflection of finished surface roughness and PTOA. Based on the model used in our experiments, the following data is used for calculation: $h_i = 0.2\ mm$ and $D = 0.4\ mm$. The data of solidification temperature, thermal conductivity and heat capacity are measured as $T_s = 166°C$, $k = 0.1745 J/(kg \cdot k)$ and $C = 1450 J/(kg \cdot k)$. The viscosity is chose as $\eta = 100 Pa \cdot s$ from literature [31]. The density of PLA is from the provider as $\rho = 1184 kg/m^3$ and the surface tension ($\sigma = 0.04 N/m$) of PLA is adopted from literature [32,33]. Substitute relevant data into Eqs.1 and 2, the results of all t_s/t_v in varying overhang angle sizes and extrusion temperatures can be calculated accordingly (see Table 5).

Table 5. t_s/t_v results in varying overhang angle sizes and extrusion temperatures.

Angle size \ Extrusion temperature	220 °C	205 °C	190 °C	175 °C
50°	0.44	0.32	0.20	0.07
40°	0.89	0.64	0.40	0.15
30°	1.88	1.35	0.83	0.31
20°	4.72	3.41	2.10	0.79

A graph was created based on Tables 3 and 5, the relationship between t_s/t_v and surface roughness can be found in this graph (see Fig. 7). As can be seen, surface roughness of overhang increases as t_s/t_v increases.

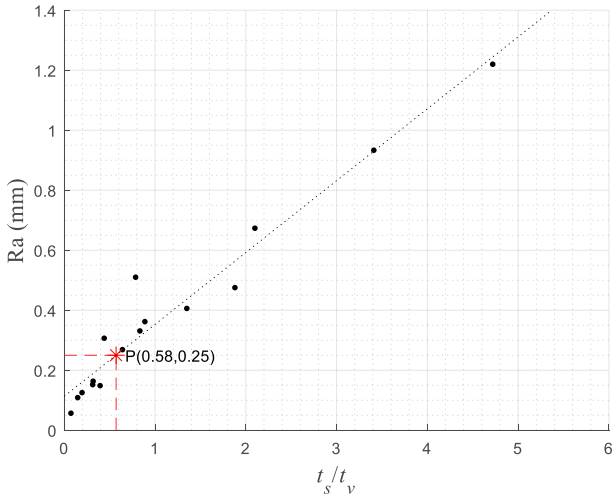

Fig. 7. Relationship between t_s/t_v and surface roughness.

Based on these findings, Eqs.1 and 2 can be used for predicting the PTOA when the properties of material are provided. Different products have different requirements of surface finish. This depends on the tolerance of a product, the PTOA can be higher if higher surface resolution is required or lower if higher surface roughness is acceptable. Limitations on acceptable surface roughness can be placed by aesthetic needs, as well as surface functionality needs, fit and assembly requirements or subsequent surface coating processes [34]. For instance, imaging surface roughness of 0.25 mm is acceptable in some case. Then, for achieving the lowest PTOA, t_s/t_v can be set at 0.58 according to the relationship between surface roughness and t_s/t_v (see Fig. 7). The lowest printable extrusion temperature (175 ℃ in this study) is better for achieving the lowest PTOA. Thus, the lowest PTOA can be set at 27° according to Eq.3.

Therefore, theoretically speaking, PTOA can be achieved at 27° when setting extrusion temperature at 175 ℃ for achieving surface roughness less than 0.25 mm in this Delta printer and this PLA material. However, the surface roughness of 175 ℃, 27° overhang is 0.261 mm according to the experiment result, which is a little different from the calculation result. This is reasonable as the calculation did not consider the environmental and other impacts. Also, the surface roughness calculated is an average value, a little higher or lower value is normal. In this case, we can set the angle size a little bit larger than the calculated size which can make sure a better surface quality and qualified products (e.g. setting the PTOA at 30°). Fig. 8 shows the satisfactory printed "UOA" part with every overhang angle of 30°. The mean surface roughness of "U" part is 0.154 mm, "O" 0.169 mm and "A" 0.175 mm. These results are also in well line with the data in the experiments (see Table 3). In the future, once the material used and its properties are known, the lowest PTOA can be calculated and predicted according to this method, thus reducing the usage of support, print time and cost.

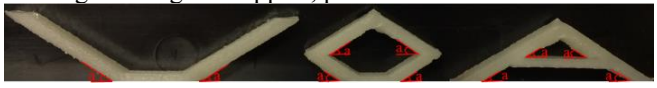

Fig. 8. Printed "UOA" part with every overhang angle of 30° (∠a=30°) in extrusion temperature of 175 ° C.

6. Conclusions

The aim of this paper is for achieving a lowest PTOA, thus reducing the use of support structure, material waste and cost. This paper theoretically and experimentally analyses an overhang structure, mainly investigates the extrusion temperature's effect on overhang surface quality and PTOA. Image-based analysis of the printed overhangs are carried out through NI vision assistant and Engauge Digitizer 4.1. t_s/t_v is used as a reflection for predicting the lowest PTOA. The findings of this research and the corresponding lowest PTOA can be integrated into slicing software for generating less support structure and saving more material, time and cost. Based on the findings of this paper, the following conclusions can be made:

●According to the results of printed overhangs in different angle sizes (see Fig. 5 and Table 3), the lower the overhang angle is, the higher the possibility of larger surface roughness could be. When the surface roughness is within tolerance (depending on the requirement of the product) in some angles, higher overhang angles do not need support while lower overhang angles do. This is also the reason why a slicing software needs to have a threshold overhang angle for generating support area.

●According to the theoretical analysis and experiment results, Eqs.1 and 2 can be used for predicting the lowest PTOA when the properties of filament material are provided. However, this depends on the tolerance of a product, the PTOA can be higher if higher surface finish is required or lower if higher surface roughness is acceptable.

●According to the results of printed overhangs in different extrusion temperatures (see Fig. 5 and Table 3), the lower the extrusion temperature is, the less the deformation will be, thus lowering PTOA. However, the printed strength/solidity/quality will be influenced by extrusion temperature [30]. Once the required extrusion temperature is known, Eqs.1 and 3 can be used for predicting the lowest PTOA, thus saving more time, support material and cost in the future, in particular producing a large number of the same products.

●For the Kossel Delta printer used in this paper, PTOA can be achieved at 30° for surface roughness less than 0.25 mm with 175 °C of extrusion temperature.

●The findings from this study can also provide some references for future research in high-precision printing.

Acknowledgements

The authors are grateful for the advices from Laboratory for Industry 4.0 and Smart Manufacturing Systems members, The University of Auckland.

References

[1] Wohlers T, Gornet T. History of Additive Manufacturing. Wohlers Report 2014 - 3D Printing and Additive Manufacturing State of the Industry 2014:1–34. doi:10.1017/CBO9781107415324.004.

[2] Jiang J, Xu X, Stringer J. Support Structures for Additive Manufacturing: A Review. Journal of Manufacturing and Materials

Processing 2018;2:64. doi:10.3390/JMMP2040064.

[3] Tang Y, Mak K, Zhao YF. A framework to reduce product environmental impact through design optimization for additive manufacturing. Journal of Cleaner Production 2016;137:1560–72. doi:10.1016/j.jclepro.2016.06.037.

[4] Jiang J, Stringer J, Xu X, Zheng P. A benchmarking part for evaluating and comparing support structures of additive manufacturing. 3rd International Conference on Progress in Additive Manufacturing (Pro-AM 2018), 2018, p. 196–202. doi:10.25341/D42G6H.

[5] Jiang J, Stringer J, Xu X, Zhong RY. Investigation of printable threshold overhang angle in extrusion-based additive manufacturing for reducing support waste. International Journal of Computer Integrated Manufacturing 2018;31:961–9.

[6] Jiang J, Xu X, Stringer J. A new support strategy for reducing waste in additive manufacturing. The 48th International Conference on Computers and Industrial Engineering (CIE 48), Auckland: 2018, p. 1–7.

[7] Jiang J, Lou J, Hu G. Effect of Support on Printed Properties in Fused Deposition Modelling Processes. Virtual and Physical Prototyping 2019. doi:10.1080/17452759.2019.1568835.

[8] Jiang J, Hu G, Li X, Xu X, Zheng P, Stringer J. Analysis and prediction of printable bridge length in fused deposition modelling based on back propagation neural network. Virtual and Physical Prototyping 2019. doi:10.1080/17452759.2019.1576010.

[9] Liu J, Ma Y, Qureshi AJ, Ahmad R. Light-weight shape and topology optimization with hybrid deposition path planning for FDM parts. The International Journal of Advanced Manufacturing Technology 2018;97:1123–35. doi:10.1007/s00170-018-1955-4.

[10] Das P, Mhapsekar K, Chowdhury S, Samant R, Anand S. Selection of build orientation for optimal support structures and minimum part errors in additive manufacturing. Computer-Aided Design and Applications 2017:1–13. doi:10.1080/16864360.2017.1308074.

[11] Morgan HD, Cherry JA, Jonnalagadda S, Ewing D, Sienz J. Part orientation optimisation for the additive layer manufacture of metal components. The International Journal of Advanced Manufacturing Technology 2016;86:1679–87. doi:10.1007/s00170-015-8151-6.

[12] Jiang J, Xu X, Stringer J. Optimization of multi-part production in additive manufacturing for reducing support waste. Virtual and Physical Prototyping 2019.

[13] Domonoky, BonsaiBrain. Support - Full Disclosure 2016. http://ifeelbeta.de/index.php/support/support-full-disclosure (accessed September 11, 2017).

[14] Hopkins PE, William R. Priedeman Jr, Jeffrey F. Bye. Support material for digital manufacturing systems. US8246888 B2, 2009.

[15] Ni F, Wang G, Zhao H. Fabrication of water-soluble poly(vinyl alcohol)-based composites with improved thermal behavior for potential three-dimensional printing application. Journal of Applied Polymer Science 2017;134. doi:10.1002/app.44966.

[16] Vaidya R, Anand S. Optimum Support Structure Generation for Additive Manufacturing Using Unit Cell Structures and Support Removal Constraint. Procedia Manufacturing 2016;5:1043–59.

[17] Dijkstra EW. A note on two problems in connexion with graphs. Numerische Mathematik 1959;1:269–71. doi:10.1007/BF01386390.

[18] Strano G, Hao L, Everson RM, Evans KE. A new approach to the design and optimisation of support structures in additive manufacturing. International Journal of Advanced Manufacturing Technology 2013;66:1247–54. doi:10.1007/s00170-012-4403-x.

[19] Lu L, Sharf A, Zhao HS, Wei Y, Fan QN, Chen XL, et al. Build-to-Last: Strength to Weight 3D Printed Objects. Acm Transactions on Graphics 2014;33:1–10. doi:Artn 97\r10.1145/2601097.2601168.

[20] Wei XR, Geng GH, Zhang YH. Steady and low consuming supporting for fused deposition modeling. Zidonghua Xuebao/Acta Automatica Sinica 2016;42:98–106.

[21] Vanek J, Galicia JAG, Benes B. Clever Support: Efficient Support Structure Generation for Digital Fabrication. Computer Graphics Forum 2014;33:117–25.

[22] Jin Y, Du J, He Y. Optimization of process planning for reducing material consumption in additive manufacturing. Journal of Manufacturing Systems 2017;44:65–78.

[23] Lee J, Lee K. Block-based inner support structure generation algorithm for 3D printing using fused deposition modeling. The International Journal of Advanced Manufacturing Technology 2017;89:2151–63. doi:10.1007/s00170-016-9239-3.

[24] Mertens R, Clijsters S, Kempen K, Kruth J-P. Optimization of Scan Strategies in Selective Laser Melting of Aluminum Parts With Downfacing Areas. Journal of Manufacturing Science and Engineering 2014;136:061012. doi:10.1115/1.4028620.

[25] Wang D, Mai S, Xiao D, Yang Y. Surface quality of the curved overhanging structure manufactured from 316-L stainless steel by SLM. International Journal of Advanced Manufacturing Technology 2016;86:781–92. doi:10.1007/s00170-015-8216-6.

[26] de Gans B-J, Duineveld PC, Schubert US. Inkjet Printing of Polymers: State of the Art and Future Developments. Advanced Materials 2004;16:203–13. doi:10.1002/adma.200300385.

[27] ARDEKANI AM, SHARMA V, McKINLEY GH. Dynamics of bead formation, filament thinning and breakup in weakly viscoelastic jets. Journal of Fluid Mechanics 2010;665:46–56.

[28] Mckinley GH. Dimensionless Groups For Understanding Free Surface Flows of Complex Fluids. Rheology Bulletin 2005;72:6–9.

[29] Representation of surface roughness in fused deposition modeling. Journal of Materials Processing Technology 2009;209:5593–600.

[30] Decuir F, Phelan K, Hollins BC. Mechanical Strength of 3-D Printed Filaments. 2016 32nd Southern Biomedical Engineering Conference (SBEC), IEEE; 2016, p. 47–8.

[31] Hamad K, Kaseem M, Deri F. Melt Rheology of Poly(Lactic Acid)/Low Density Polyethylene Polymer Blends. Advances in Chemical Engineering and Science 2011;01:208–14.

[32] Yixiang Xu MAH. Electrospray encapsulation of water-soluble protein with polylactide: Effects of formulations on morphology, encapsulation efficiency and release profile of particles. International Journal of Pharmaceutics 2006;320:30–6.

[33] Wang S, Cui W, Bei J. Bulk and surface modifications of polylactide. Analytical and Bioanalytical Chemistry 2005;381:547–56.

[34] Turner BN, Gold SA. A review of melt extrusion additive manufacturing processes: II. Materials, dimensional accuracy, and surface roughness. Rapid Prototyping Journal 2015;21:250–61.